Original Article

Institution of MECHANICAL ENGINEERS
Journal of MECHANICAL ENGINEERING SCIENCE

Proc IMechE Part C:
J Mechanical Engineering Science
0(0) 1–15

DOI: 10.1177/0954406220970595
journals.sagepub.com/home/pic
SAGE

Inverse thermal modeling and experimental validation for breast tumor detection by using highly personalized surface thermal patterns and geometry of the breast

O Mukhmetov[1], A Mashekova[1], Y Zhao[1], EYK Ng[2], A Midlenko[3], S Fok[1] and S.L Teh[1]

Abstract

Infrared (IR) Thermography is currently a supplementary technique for breast cancer diagnosis. There have been studies using IR thermography and numerical modeling in an attempt to detect tumor inside the breast. Most of these studies focused on either the "forward modeling" problem or only used idealized or population-averaged patients' data, whereas identification of the tumor inside the breast based on the thermal pattern is an "inverse modeling" problem dependent on personalized information of the patient. Inverse modeling is based on the idea that the surface thermal pattern of the breast can be used to determine the tumor features based on physical and physiological principles. The current study aims to develop a well-validated inverse thermal modeling framework that could be used to determine the depth and size of tumor inside a breast based on personalized patients' breast data, such as thermogram and 3D geometry using efficient design optimization techniques and Finite Element Modeling (FEM) to support the process. The numerical modeling was validated by the experiments, conducted using artificial breasts. Results show that although DIRECT Optimization method can be employed to find the depth and size of the tumor with good accuracy, the technique can be very time consuming. On the other hand, Response Surface Optimization method is also able to find the depth and size of the tumor with less accuracy but faster when compared with DIRECT Optimization. The last method tested, Nelder-Mead method, failed to detect the tumor. The study concludes that Response Surface Optimization method should be used first, and after the range of parameters are found, the DIRECT optimization method can be applied for more accurate results. However the GA method was found to be the only viable and efficient design optimization method for reverse modeling when blood perfusion was adopted in the breast model and many parameters were searched for with patient specific data input for breast tumor diagnosis.

Keywords

Inverse modelling, breast tumor, thermal patterns, thermography, direct optimization, response surface optimization

Date received: 9 March 2020; accepted: 11 October 2020

Introduction

Breast cancer is acknowledged as a major disease among female population. To reduce the prevalence of the breast cancer and mortality rates, the detection of the disease at its earliest stage is vital.[1–13] According to the American Cancer Society, breast cancer is one of the most common cancer among young people at the age between 20 to 39.[2]

The gold standard for breast tumor detection is mammography. This method of detection is mostly used for women over the age of 40. It is less effective for younger women because of the radiation risk and

[1]Department of Mechanical and Aerospace Engineering, School of Engineering and Digital Sciences, Nazarbayev University, Nur-Sultan, Kazakhstan
[2]School of Mechanical and Production Engineering, Nanyang Technological University, Singapore, Singapore
[3]Department of Medicine, School of Medicine, Nazarbayev University, Nur-Sultan, Kazakhstan

Corresponding author:
A Mashekova, Department of Mechanical and Aerospace Engineering, School of Engineering and Digital Sciences, Nazarbayev University, 53 Kabanbay batyr Avenue, Nur-Sultan 010000, Kazakhstan.
Email: aigerim.mashekova@nu.edu.kz

density of the breast. In addition, mammography cannot be used for nursing and pregnant women due to x-ray radiation.

An alternative and non-invasive method of breast cancer detection is infrared thermography. It is a portable, sensitive, non-invasive, non-radiating, and cheap method for the early detection of the tumor in the breast. The study by Gautherie and Gros[3] concluded that breast cancer could be better diagnosed at an earlier stage if the gold standard methods are combined with thermography. Thermography could be considered as a supplementary method to mammography for the early detection of breast cancer, particularly in dense breasts, where mammography could have high false-positive results.

The basic principal of the infrared thermography (IRT) to diagnose the tumor in the breast is that blood flow to the tumor is found to be higher compared to the normal tissues in a breast. The tumor cells have increased metabolic activity, and therefore the temperature of the tumor tissue is higher compared to the normal tissue. Thermography can identify the temperature increase in the tissue, which is reflected on the surface of the breast. The color distribution of the thermogram for the surface of the breast will show any abnormalities of the internal temperature distribution. Any existence of obvious surface hot spots, as well as asymmetrical distribution of the temperature of the two breasts could pinpoint to the existence of the tumor (except the water based cysts) inside the breast.

Although thermography has simple working principle, the diagnosis is predicated based on qualitative principles and human judgement, for example, asymmetry of two breasts, hyperthermetic patterns and abnormal vascular patterns.[4] Quantitative information is usually manually extracted by observing the temperature distribution and randomly matching the temperature profiles at different locations. With the rapid development of computer technologies, computer-aided tools can be used to support the interpretation of thermal images and help doctors to automatically identify location and size of the tumor, blood perfusion and other personalized properties of the breast tissues, and thus assist with the diagnosis.

The problem of the tumor size and location identification based on IR thermography is related to the so-called "inverse thermal problem". There were a few studies,[5–10] that made contributions to solve the breast cancer "inverse problem". Mitra and Balaji[5] presented a method of using artificial neural network and genetic algorithm to evaluate the tumor metabolic heat generation, location and size by using 2D multilayer model of the breast. A similar study by Tepper et al.[6] explored steady state analysis based on the artificial neural network method to estimate tumor size, metabolic heat generation and location of the affected area using a 3D single layer breast model. Research reported by Bezerra et al.[7] incorporated two types of geometry. The first, a 3D breast geometry used as a human phantom and obtained from a female mannequin. The second substitute geometry was obtained by scanning seven different breast external prostheses, manufactured by Orto Pauher. The Coordinate Measuring Machines (CMM) was used to acquire the point coordinates over the breast surface. The second substitute geometry was obtained using seven different breast external prostheses were scanned: models SG-419 and SG-420, with sizes 1, 2, 4, 6, 8, 10 and 12, manufactured by Orto Pauher which donated all the prostheses. The CMM measured the prostheses. There are two other studies[8,9] that explored the genetic algorithm and curve fitting methods to define the location of the tumor and the size by using 2D rectangular single layer breast model. These works were developed based on the 3D hemispherical breast model for steady-state analysis. Studies[4,10] conducted steady state and transient analysis by using Lavenberg-Marquard method to simultaneously estimate multiple properties of the breast tissue. These studies showed that transient analysis is more appropriate for the tumor stage evaluation using blood perfusion based on the temperature distribution.

In this paper we aim to develop a well-validated inverse thermal modeling framework that could be used to determine the depth and size of tumor inside a breast based on personalized patient's breast data, such as thermogram, 3D geometry and tissue properties, using efficient design optimization techniques and Finite Element Modeling (FEM) to support the process. The tumor parameters were evaluated using optimization tools in ANSYS and COMSOL software and validated by experiments with artificial breasts.

Methodology

The inverse determination of tumor parameters, such as size and location, based on the surface temperature of the breast consists of several steps. The procedure starts from the scanning of the breast's geometry to build its 3D model. The obtained geometry was used to build not only the 3D geometry for the numerical part of the study, but also the artificial breast for the experiment. Experiments on the artificial breast were conducted to generate the breast surface temperature data for validating the inverse modelling findings. In the experiment the surface temperature was obtained by using Thermal Camera IRTIS 2000. The camera has a spectral range of 3–5 μm, measured temperature range of $-20\,^{\circ}C$ to $+300\,^{\circ}C$, margin of error $\pm 1\,^{\circ}C$, temperature sensitivity of $0.02\,^{\circ}C$, frame resolution 640×480, heterogeneity throughout the frame of no more than $\pm 0.1\,^{\circ}CC$, temperature resolution across the entire field of view $0.05\,^{\circ}C$ ($0.02\,^{\circ}C$), spatial resolution 1.5 mrad, field view 25×20 deg, frame time 0.8 sec, 1.6 sec, 3.2 sec. These thermograms were used (as boundary conditions) for the forward

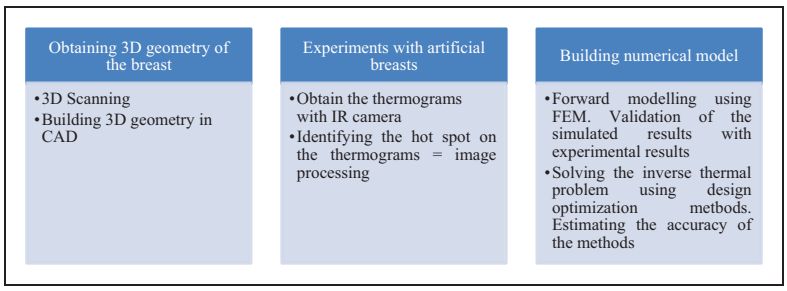

Figure 1. Methodology of the study.

modelling. After the forward model had been validated and temperature patterns and temperature probes were gathered, they were used as input data for the reverse modelling (Figure 1).

To build the 3D geometry of the artificial breast, the 3D Scanner ZScanner700 was used. A dummy size of $800 \times 838 \times 635$ mm with both breasts was scanned (Figure 2) and the obtained solid model was then processed in SolidWorks (Figure 3). The 3D breast geometry and its STL file were generated. The data was used to 3D-print the molds for the artificial breasts (Figures 3 and 4), as well as creating the 3D geometrical models for finite-element analysis. The artificial breasts were made of Dragon Skin 10 Medium Set Silicone Rubber. During the artificial breast molding, resistors and wires were inserted into the breast at pre-defined X, Y and Z-coordinates (Figure 5). Embedded resistors have a cylindrical shape with the length and diameter of 6 and 2 mm, respectively. The volume of a resistor can be calculated as: $V = \pi r^2 h = \pi \times 1^2 \times 6 = 18.9\ \text{mm}^3$.

The detailed information about the locations and sizes of the artificial tumors could be found in Table 1.

In order to observe the temperature distribution on the surfaces of the artificial breasts, an infrared thermographic camera IRTIS 2000 was employed. The camera can determine the temperature values at any point and the location of the interested temperature point can be obtained using the IR camera software (Figure 6).

Pre-defined hot spots were used as temperature probes in ANSYS and COMSOL, which were utilized as tools for the numerical simulation. Table 2 shows the temperature probes coordinates.

In order to perform the inverse thermal simulation, FEM models were created in ANSYS and COMSOL. The model includes 3D geometries of the breast and tumor, and the locations of the probes, as well as the initial search location for the tumor. The following information were assumed and pre-defined: initial temperature of the breast equal to the ambient temperature 24 °C, the thermal conductivity was 0.16 *W/m-K*, and the heat generation value was dependent on the size of the tumor shown in Table 1. Figure 7 shows the 3D geometry of the breast, which was modeled in SolidWorks, and input into ANSYS for FEM meshing.

Figure 2. Dummy breast, prepared for scanning.

Mathematical modeling

For forward mathematical modeling, Pennes' bioheat equation was used. Equation (1) presents the relationship between temperature, thermal conductivity, heat capacity, volumetric metabolic heat generation rate and influence of the blood perfusion on the temperature distribution based on the energy conservation principle:[14]

$$\rho c \frac{dT}{dt} = \nabla \cdot (k \nabla T) + \rho_b w_b c_b (T_a - T) + q_m \qquad (1)$$

where T (°C) is temperature of the tissue, which is equal to 37 °C, as the temperature of the core body; k is the thermal conductivity of tissue ($W/m{\cdot}K$) equals to 0.16 W/m-K; ρ is the density (kg/m^3), which is equal to the density of the silicone, used in the artificial breasts for the experiments; q_m is the metabolic heat generation per unit volume (W/m^3) which depends on the size of the tumor. Next part of the equation describes the influence of the blood perfusion w_b on the temperature distribution in the breast, which is in the case of study was equal to zero, as the conducted experiments were based on the single layer model without considering the blood perfusion rate. T_a represents the temperature of arterial blood (°C); c is the

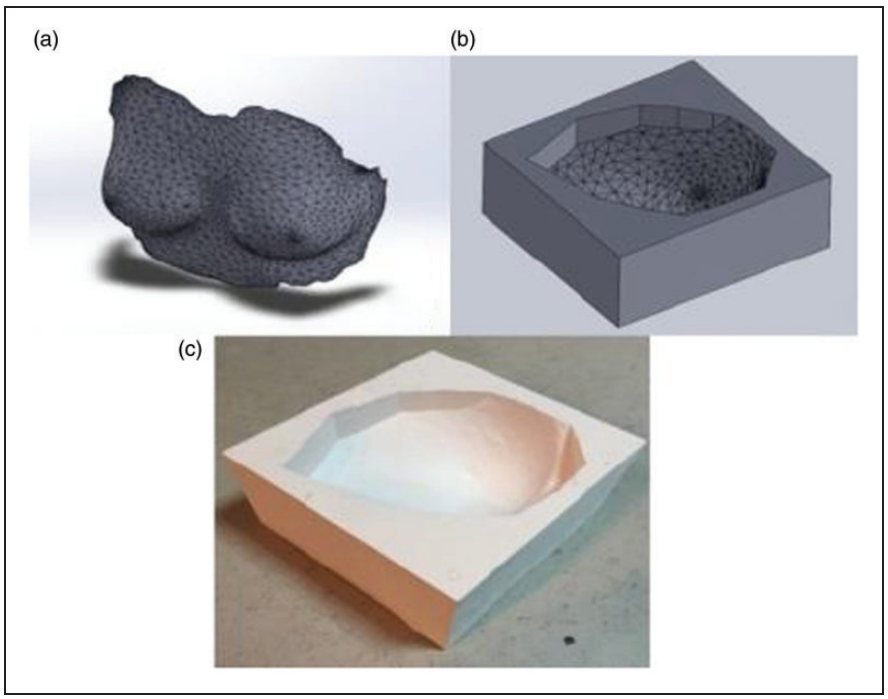

Figure 3. (a) Scanned image; (b) 3D image of the mold created in CAD; (c) Mold manufactured by the 3D printing.

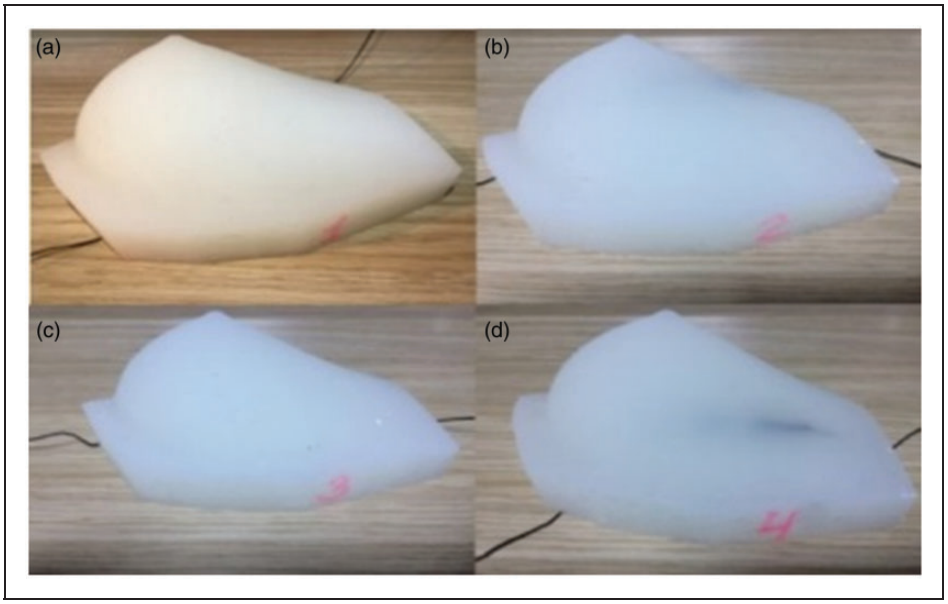

Figure 4. Silicone Breasts with different locations and size of the artificial tumor: (a) 75.4 mm^3; (b) 150.8 mm^3; (c) 113.1 mm^3; (d) 75.4 mm^3

specific heat ($J/Kg\cdot{}^{\circ}C$); C_b is the specific heat of the blood (kg/m^3). The main assumptions of the above model are homogenous properties in terms of breast tissue density and conductivity.

The left hand side of equation (1) represents the rate of change of the temperature in the tissue. However, in the current research the thermal analysis was conducted in steady-state condition, therefore the Penne's equation (1) will take the form:

$$k\nabla^2 T + \rho_b c_b w_b (T_a - T) + \dot{q_m} = 0 \tag{2}$$

Mathematical modeling also includes prescribing boundary conditions to the model, therefore the model includes boundary conditions such as surface heat convection (3) and boundary temperature (4).

$$-k\,\nabla T = h(T_s - T_a) \tag{3}$$

$$T_s = T_a \tag{4}$$

where h ($W/m^{2}\cdot{}^{\circ}C$) is convective heat transfer coefficient and equal to 13.5 $W/m^{2}\cdot{}^{\circ}C$, that was established

by the experiments; T_s is surface temperature; T_a is ambient temperature.

Taking into account equations (2) and (3), the Penne's bio-heat integral equation for the Finite Element Model is as follows:[15]

$$\iiint_V k_x \frac{\partial W_1}{\partial x}\frac{\partial T}{\partial x} + k_y \frac{\partial W_1}{\partial y}\frac{\partial T}{\partial y} + k_z \frac{W_1}{\partial z}\frac{\partial T}{\partial z} - \left(Q_m W_1 + \rho c \frac{\partial T}{\partial t} W_1\right) \mathrm{d}v + \oiint_S h_c (T - T_e) W_1 \mathrm{d}s = 0 \quad (5)$$

where V is the volume integral; S is surface integral range; W_1 is the weighting function.

Design optimization methods were used to find the depth and size of the tumor so that the temperatures predicted by the FEM thermal model match those at six probes.

Design optimization methods for reverse thermal modeling

In the current study, the design optimization methods aim to search for a set of optimal data, including tumor sizes and locations to minimize the difference between the given thermogram and predicted temperature of the forward FEM thermal model.[16,17]

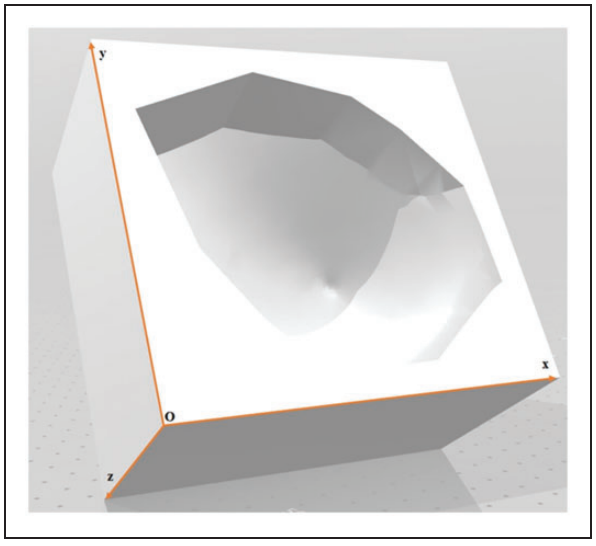

Figure 5. X, Y, Z axis of the coordinate system.

Thus, according to Baeyens et al.[17] f is the function that should be minimized, whereas the search space is unit n-box $(0,1)^n$. The main goal is to identify a value $x^* \in (0,1)^n$, in a way the f function reach minimum at x^*. Therefore, when f *is* continuously differentiable in $(0,1)^n$, then:[17]

$$\nabla f\,(x^*) = 0, \;\; x^* \in (0,1) \quad (6)$$

The objective function is the temperature difference between the same probes obtained during the experiment and computational study. Goal of the optimization is to minimize temperature difference between experimental and computational model by searching for the right size and depth of the tumor.

There are a number of DIRECT search methods to solve the problem. Modern methods do not need any gradient information about the function.[16–18] The principle of the DIRECT search algorithm is that it looks for the set of the points around the current point, and thus finding the one that has lower value among these points. There are two types of optimization: local and global optimizations. The local optimization is appropriate for convex problems. However, it is difficult to justify that the defined local optimum is global. The second method is in fact derivative free methods which have two classes of implementation algorithms in global optimization. One of them is Lipschitz optimization methods, described in literature.[19–22] The main idea is to use cost functions for auxiliary functions, whereas the last function is semi-linear and calculated by segmentation of the search space and continuously using the Lipschitz property.[19–22] One of the methods of this class is DIRECT, that is described in Jones et al..[23]

The name of DIRECT optimization is derived from "DIviding RECTangles" and the name describes the way this method works. DIRECT works by segmenting rectangles into smaller rectangles, and after which smaller rectangles are trisected and the center points of the outer thirds are selected. The main part of the method is the identification of the rectangles, as it determines the way the search efforts are implemented over space.[24,25] Thus, this method was founded with the aim to find solutions

Table 1. Heat source data.

Numbering of breast as in Figure 4(a) to (d)	1	2	3	4
Location of the artificial tumor (mm)				
X	92	95	145	60
Y	89	100	80	100
Z	35	54	40	45
Quantity of the resistors	4	8	6	4
Total volume of the heat sources, mm^3	75.4	150.8	113.1	75.4
Volumetric heat generation rate, W/m^3	0.0037	0.00015	0.00373	0.00223

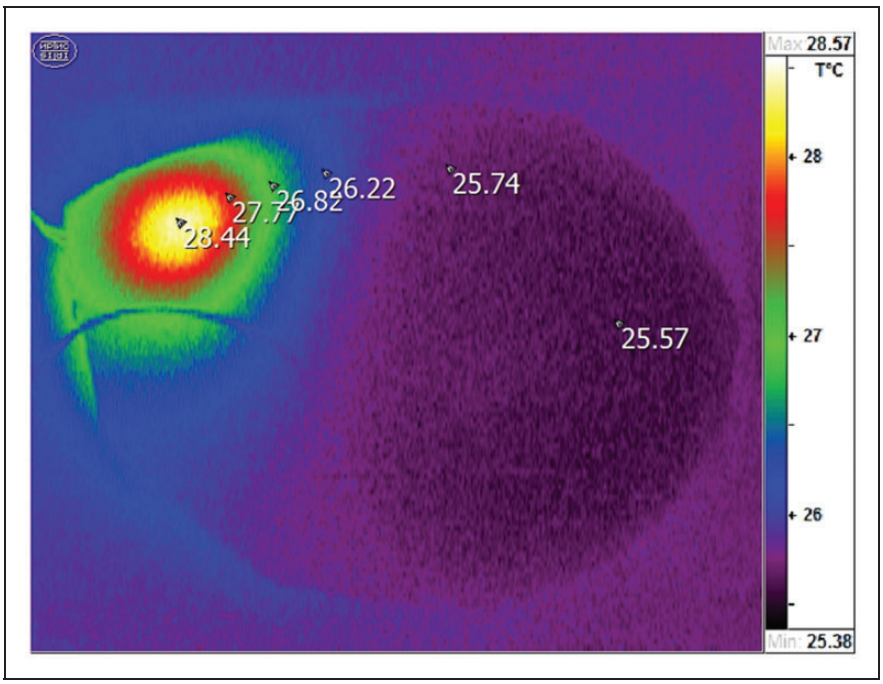

Figure 6. Thermal image of the breast No. 2.

Table 2. The coordinates of the temperature probes.

Probe	X (*mm*)	Y (*mm*)	Z (*mm*)
1	134.91	43.45	50
2	137.33	58.80	52
3	136.24	71.40	55
4	134.91	86.80	57
5	125.14	120.07	63
6	68.33	150.81	69

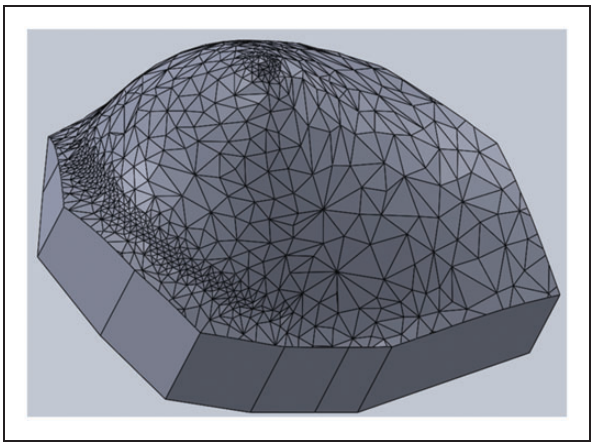

Figure 7. 3D geometry of the breast with FEM surface meshing.

for the difficult global optimization problems without closed form functions, and at the same time it does not require any information on the objective function gradients. In other words, it is a random sampling method, which selects points in space and then employs the points in order to define where to search next. According to literature[24,25] this method has become very popular and competitive.

The Genetic Algorithm (GA) is based on biological evolutionary theory and numerically applied to optimization problems. Algorithm was developed at University of Michigan by Johny Holland.[26] Fundamental of GAs technique borrowed from "survival of the fittest" Darwin's principle. The beneficial characteristic to survival of biological species evolve, tend to pass through genetics, so that individuals gain opportunity for future breed. The concepts of this natural processes as, reproduction, crossover and mutation successfully applied on solving optimization and search problems.[27]

Another mathematical and statistical method that was used for the tumor size and depth estimation is **Response Surface Optimization Method**. The idea of the method is to estimate output variable, which is the surface response, based on the input data.[28] The response surface model is a continuous process, which builds an approximate model, by using a sequence of designed experiments and polynomial functions to obtain an optimal response. In the case of optimization of the tumor parameters in a breast, the objective is to find the depth (x_1) and the size (x_2) of the tumor in the breast, or the location of the tumor in terms of X (x_1) and Y (x_2) coordinates, that can generate the temperature distribution on the surface of the breast (y). Therefore, it gives the following function:[28]

$$y = f(x_1, x_2) + \varepsilon \tag{7}$$

where ε is the noise or error observed in response y; $f(x_1, x_2)$ is a response surface.

The third method that was used for searching the depth and size of the tumor was Nelder-Mead method,[29] which is a pattern search and derivative-free local method in mathematics, belonging to the class of simplex-based direct research methods. This method was described by Spendley et al.[29,30] and based on the principal of a pattern set of $n + 1$ vectors. Moreover the method is based on five processes: reflection, expansion, outer contraction, inner contraction and shrinkage, which are used one by one during each iteration. The numerical simulation conducted based on this method was implemented in COMSOL. The Nelder-Mead algorithm starts by ordering the vertices of the simplex and uses the above five operators: reflection, expansion, outer contraction, inner contraction and shrinkage. At each iteration only one of these operations is performed. As a result, a new simplex is obtained such that either contains a better vertex or has a smaller volume

The fourth method is Canonical Genetic Algorithm (CGA) which is a simple version of GA, originally developed by Holland.[31] The principle of the algorithm is to find global optimal parameters that meet requirements by crossover and mutation with a proportional selection operator. Figure 8 presents the concept of CGA procedure.

The first step is initialization, where the first population is generated randomly. From this population individuals x_i are picked, depending on their probability to breed next generation. The probability is calculated by relation of individual and total fitness values f:

$$P\{x_i \ is \ selected\} = \frac{f(x_i)}{\sum_{j=1}^{m} f(x_j)} > 0$$

The second step is to crossover selected individuals. Let's suppose chromosome with length l, and pick random number c from 1 to l. The first child's chromosome is formed, from the first c elements of 2nd parent, and last l – c elements of 1st parent. For the second child, procedure is vice versa. An example is shown below:

Parent 1	1001|010010	Child 1	0101 010010
Parent 2	0101|111011	Child 2	1001 111011

The last step is to implement mutation on each child's chromosome. A random number v is generated between 1 and l, so that the v-th element randomly changes to 0 or 1, with probability range from 0.001 to 0.01. The above procedure as shown in Figure 8 is repeated till fitness value is met.[31]

Mesh verification

In order to perform mesh verification study, the second breast was used. The tumor size was 5.77 mm in diameter, with a heater power of 0.0031 W. There was set of 3 temperature probes, whose locations are shown in Table 3. The number of elements was increased from mesh one to mesh four as shown in Table 6, which show that mesh convergence can be achieved with mesh 3 and thus was used as the optimal one in subsequent studies.

The temperature difference between studies number 3 and 4 is 0.001, so that 3rd mesh was decided to be used for further simulations (Table 4).

Results and discussion

Forward numerical modeling was first conducted to validate the numerical model with experiments. Forward modeling was implemented by solving Pennes' equation and applying boundary conditions (3) and (4) with ANSYS Mechanical FEM.

The results obtained during forward modelling confirm that the thermal model can be used to predict the distributions of surface temperatures of the breasts (Figure 9). The sizes and the locations of tumors inside the breasts are indicated in Figure 4 and Table 1.

The obtained experimental results can also be used for inverse thermal simulation studies, i.e. to determine tumor locations and sizes based on breast surface temperature distributions from input thermograms (Figure 6). Knowing the temperature distribution on the surface of the breast the inverse numerical simulation should determine the depth and the size of the tumor using design optimization methods.

First, the DIRECT optimization method was used to estimate the depth and size of the tumor. For validation purpose the obtained results were compared with the experimental results.

Figure 10 presents the convergence history of the DIRECT method. The process fluctuates in its initial stages while searching the design space under the defined boundaries and finally converges to the searched results. The overall convergence for the DIRECT optimization method took five hours. The computer used for the modelling has following specification: ASUS, INTEL Core i7-7700HQ CPU, 2.81 GHz, CPU $\times 64$.

Experimental data that was used for the optimization included tumor depth of 41.8 mm and tumor size of 6.6 mm. Conducted optimization showed three best candidates for the estimated depth and size of the tumor, which best fit the boundary conditions and input data. The first candidate had an estimated depth equal to 40.99 mm, the second was 39.3 mm, and the last candidate equaled to 43.48 mm. Thus, comparison of the numerical results with the experimental showed lowest error of 1.95%.

The same procedure was followed to search for the size of the tumor. The obtained results showed that the estimated size of the tumor was the

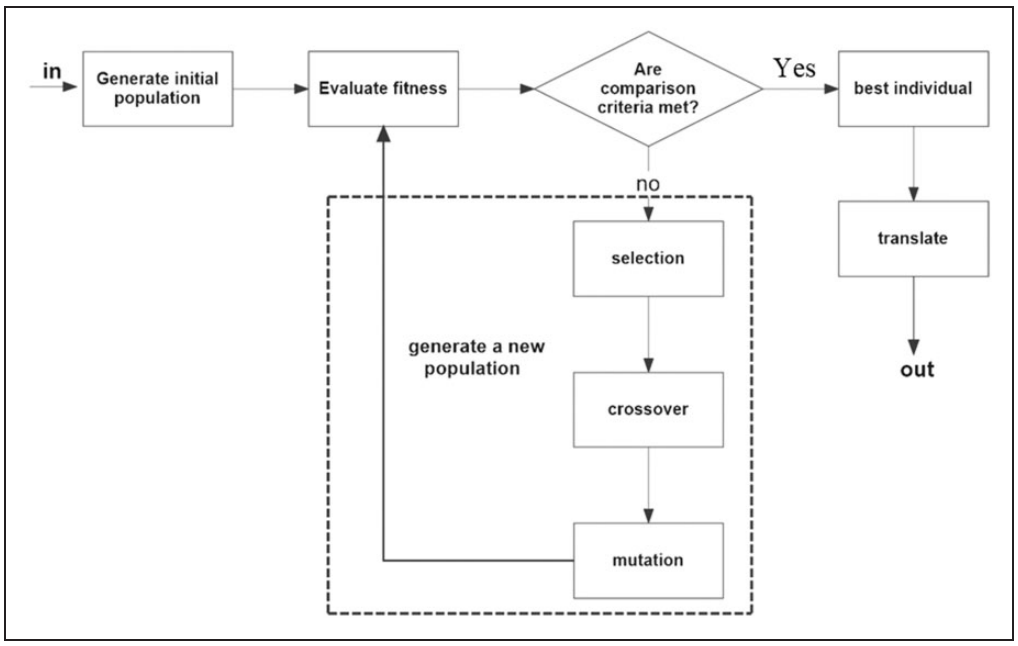

Figure 8. Standard procedure of a canonical genetic algorithm.[31]

Table 3. Temperature probes positions.

Coordinates	Probe 1	Probe 2	Probe 3
x	100	100	110
y	95	95	95
z	–56.77	–25.23	41

following: candidate one – 6.31 mm, candidate two – 6.47 mm, and candidate three – 6.14 mm, whereas the experimental size was equal to 6.6 mm. Thus, the estimated error of the numerical and experimental is equal to 1.9%.

Furthermore, the temperature at probes 1 and 2 were also optimized by following the same procedure. The results obtained during the optimization indicated, that candidate one has 28.41 °C at probe one, 27.84 °C at probe two and 26.99 °C at probe three; whereas candidate two had 28.44 °C at probe one, 27.87 °C at probe two and 27.01 °C at probe three; finally candidate three has 28.38 °C at probe one, 27.82 °C at probe two and 27.03 °C at probe three. Whereas the experimental results showed 28.44 °C at the same place as probe one, 27.77 °C at the same place as probe two and 26.94 °C at the same place as probe three. The comparison of the experimental results and estimated reverse modelling results indicated that the range of the errors to predict the temperature could be between 0 to 0.35% (Table 5).

For the Response Surface Method, the same procedure was used as for the DIRECT method. The experimental value for the depth of the tumor was 41.8 mm. The response surface optimization method defined three best fit candidates with respect to the boundary conditions of the model and input data.

Table 4. Mesh verification study.

#	No. of nodes	No. of elements	Probe 1 (K)	Probe 2 (K)	Probe 3 (K)
1	120071	40052	298.67758	298.649524	298.665518
2	246679	75813	298.370663	298.65335	298.667811
3	1217332	356437	298.368102	298.649454	298.665774
4	3331157	957479	298.368081	298.649561	298.665669

Three defined candidates for the depth were: candidate one – 40.45 mm, candidate two – 42.07 mm, and candidate three – 42.78 mm. The comparison of the experimental values and the predicted results through the response surface optimization produced the smallest error of 0.63%.

The size of the tumor was estimated by using the response surface optimization, which generated the following results: candidate one – 6.29 mm; candidate two – 6.13 mm; candidate three – 6.11 mm; whereas the experimental result was 6.6 mm. Therefore, the determined error of the size of the tumor was 4.67%.

Furthermore, the estimated temperature for three candidates at probes 1, 2 and 3 revealed that candidate one at probe one equaled to 28.36 °C, at probe two equaled 27.8 °C and at probe three 27.99 °C; whereas candidate two had the temperature at probe one – 28.32 °C, at probe two – 27.77 °C, and probe three – 27.96 °C; finally, candidate three was equaled to 28.35 °C at probe one, 27.8 °C at probe two and 27.99 °C at probe three. The experimental temperature in this case was equal to 28.35 °C at probe one, 27.8 °C at probe two and 27.99 °C at probe three. Thus, the comparison of the experimental values showed the lowest error of 0% for the

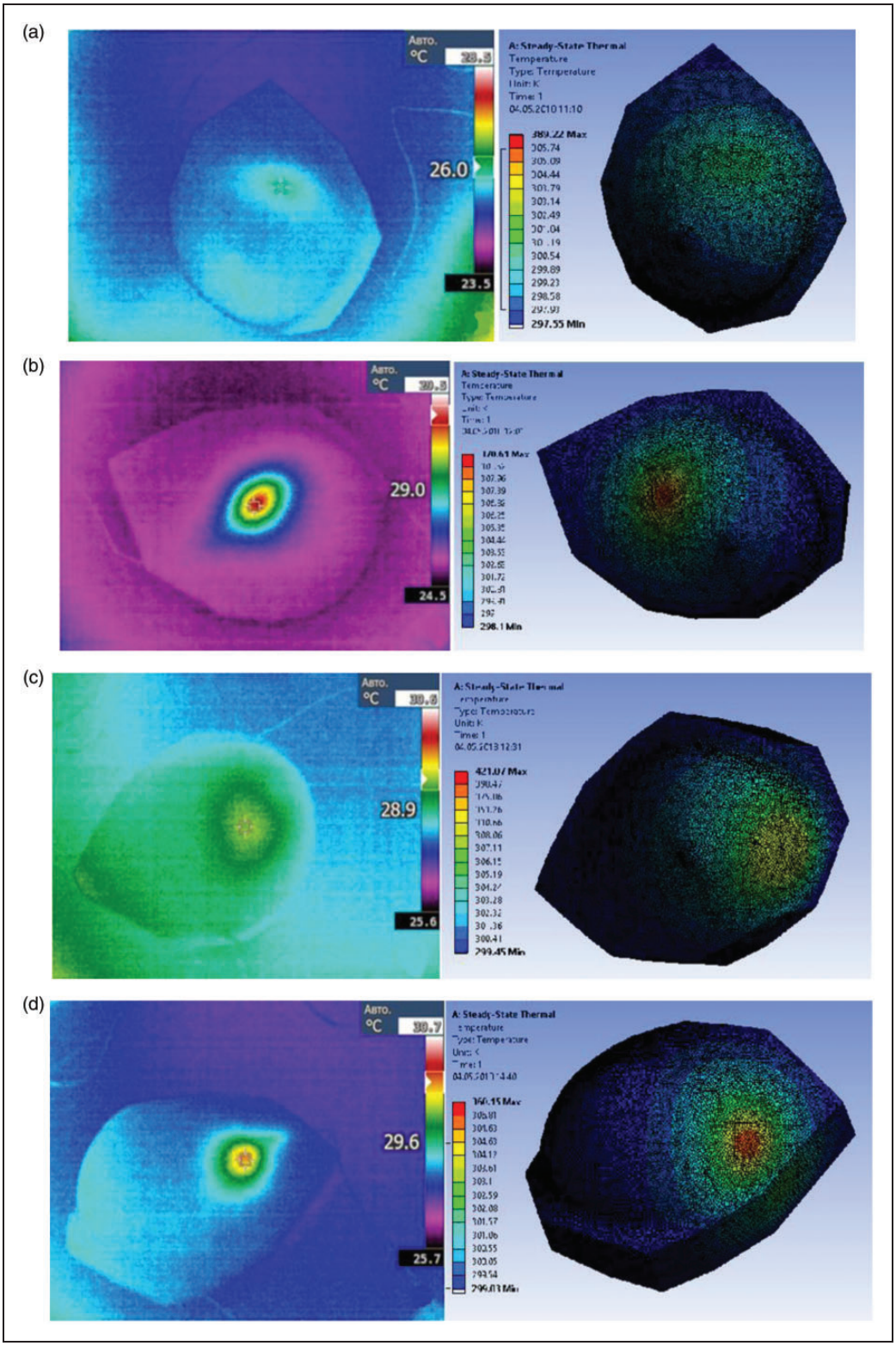

Figure 9. Validation of temperature distribution in experiment and numerical modelling: (a) breast 1; (b) breast 2; (c) breast 3; (d) breast 4.

probe two of candidate 2 and 0.43% for probe one of candidate two. Table 5 shows the tabulated data of the abovementioned results.

Figure 11 presents the convergence process of the Response Surface Optimization (RSO) method, and it can be seen, that the process starts building the approximation model, and then based on this model it decreases the search space and find the optimal parameters based on the input variables. Overall, the convergence process took 30 minutes, however this method is less accurate than the DIRECT method.

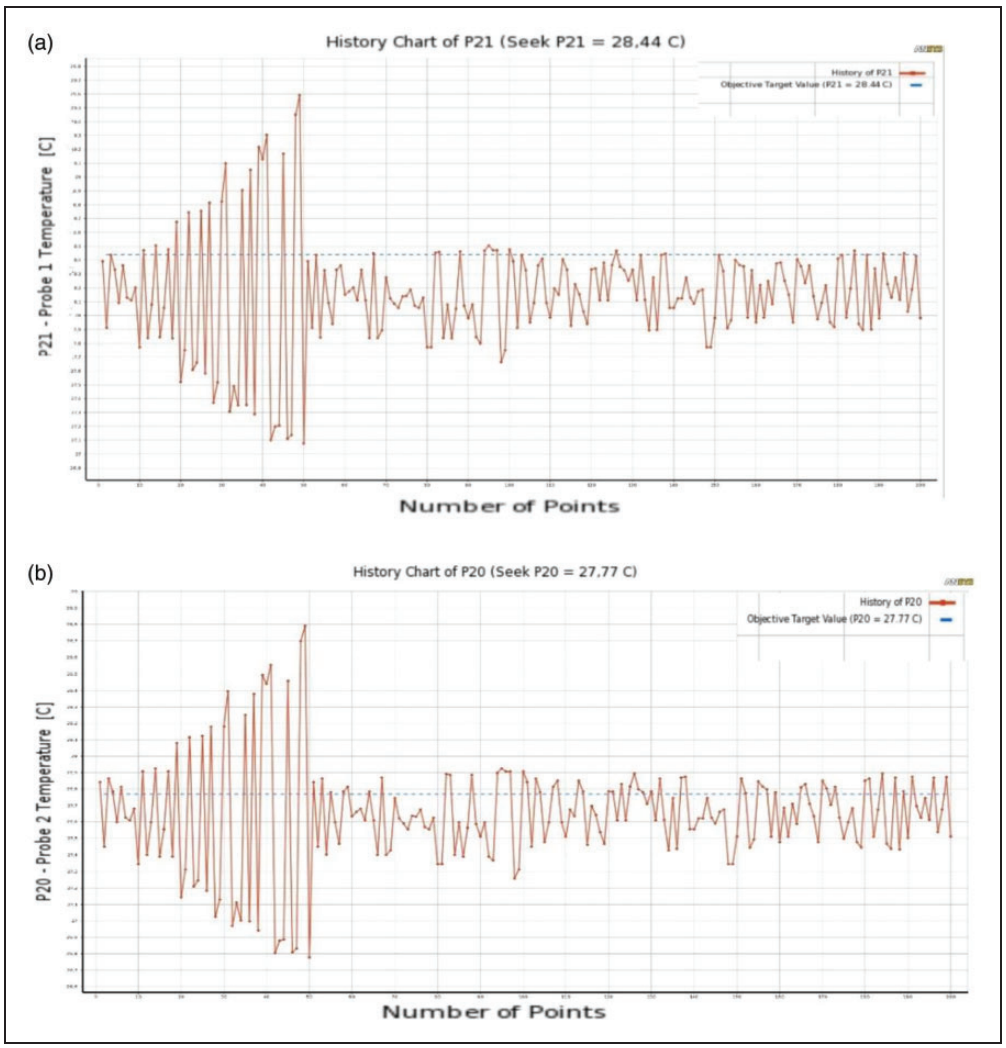

Figure 10. Temperature values at every point during the convergence process of DIRECT optimization method: (a) probe 1; (b) probe 2.

Table 5. Results of the inverse engineering.

			Candidate 1		Candidate 2		Candidate 3	
Method	Parameters	Experiment	Result	Error (%)	Result	Error (%)	Result	Error (%)
Direct Optimization	Depth (mm)	41.8	40.99	1.95	39.3	5.98	43.48	4.03
	Size (mm)	6.6	6.31	4.33	6.47	1.9	6.14	6.99
	Probe 1 (°C)	28.44	28.41	0.11	28.44	0.0	28.38	0.21
	Probe 2 (°C)	27.77	27.84	0.25	27.87	0.35	27.82	0.18
	Probe 3 (°C)	26.94	26.99	0.19	27.01	0.27	27.03	0.32
Response Surface Optimization	Depth (mm)	41.8	40.45	3.23	42.07	0.63	42.78	2.34
	Size (mm)	6.6	6.29	4.67	6.13	7.08	6.11	7.41
	Probe 1 (°C)	28.44	28.36	0.3	28.32	0.43	28.35	0.31
	Probe 2 (°C)	27.77	27.8	0.12	27.77	0.0	27.8	0.11
	Probe 3 (°C)	27.93	27.99	0.25	27.96	0.1	27.99	0.21

The third method, the Nelder-Mead method was applied for searching the depth and size of the tumor. The results obtained, indicated that the search was stuck at a local minimum, since the depth had not changed after 500 iterations as seen in Figure 12. Therefore, this method was not selected for further inverse thermal modeling.

The two methods, i.e. DIRECT Optimization and Response Surface Optimization were used in the

inverse modeling studies and the findings were validated by the experimental results.

The aim of the simulations was to find the depths and the sizes of the tumors. For that purpose the above two methods (DIRECT and Response Surface Method) were explored to find out the most appropriate for the breast cancer diagnosis. The performances of the two methods were compared in Figure 13.

The findings are tabulated and compared to the experimental results in Table 5. The calculated errors of the findings presented in Figure 13 and summarized in Table 5 led to the outcome that the DIRECT Optimization Method gives better results in terms of the approximation of the possible tumor depths and tumor sizes. But, it took around five hours for the inverse modelling to search for the parameters. On the other hand, the Response Surface Optimization method only needed thirty minutes in the inverse simulation to find the optimal set. However, the results validation indicates high inaccuracy of the simulation. Therefore, the DIRECT optimization is preferred for the inverse modelling, but the computational time does not allow us to use this method extensively. The study suggests using the Response Surface Optimization method first, and after the range of parameters are found, the DIRECT optimization method can be applied for results that are more accurate.

Table 6. Comparison of estimated parameters with doctor's diagnosis.

Patient number	Computed diameter (mm)	Doctor's size (mm)	Computed depth (mm)	Doctor's depth
1	29.89	25	29.06	Not given
2	7.98	5	6.16	Near surface

Reverse simulation for search of depths and sizes of tumor using patient specific data

Recently the collection of patients' data have been started (despite the Covid challenges) in the Oncological Center of Nur-Sultan city, Kazakhstan. From doctor's investigation it was found that two

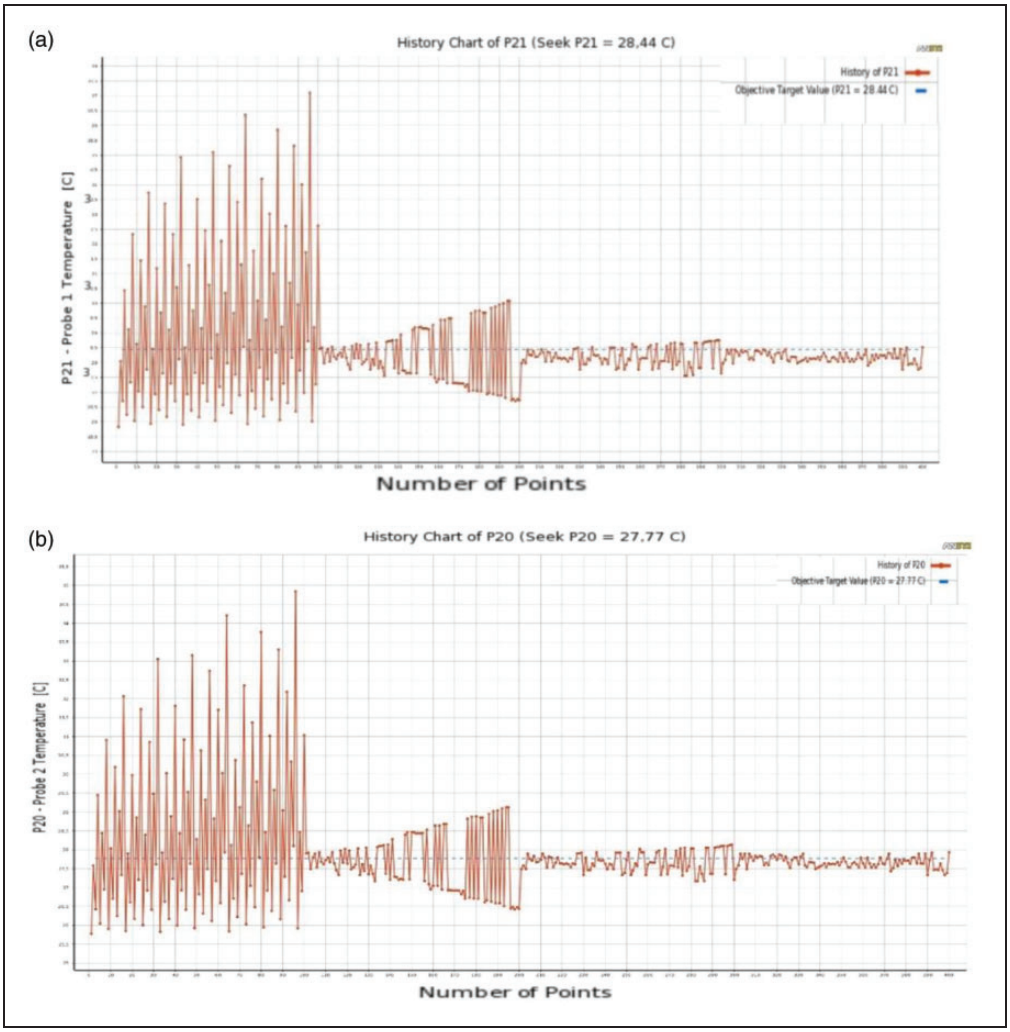

Figure 11. Temperature values at every point during the convergence process of RSO method: (a) probe 1; (b) probe 2.

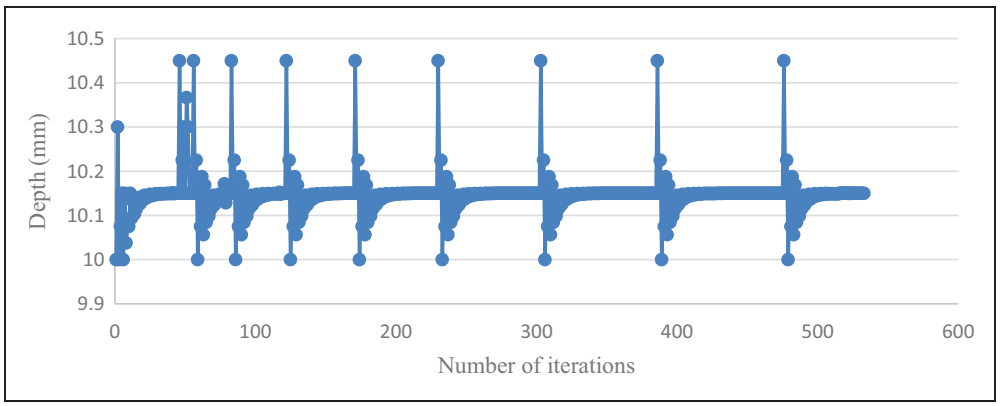

Figure 12. Depth distribution from iteration.

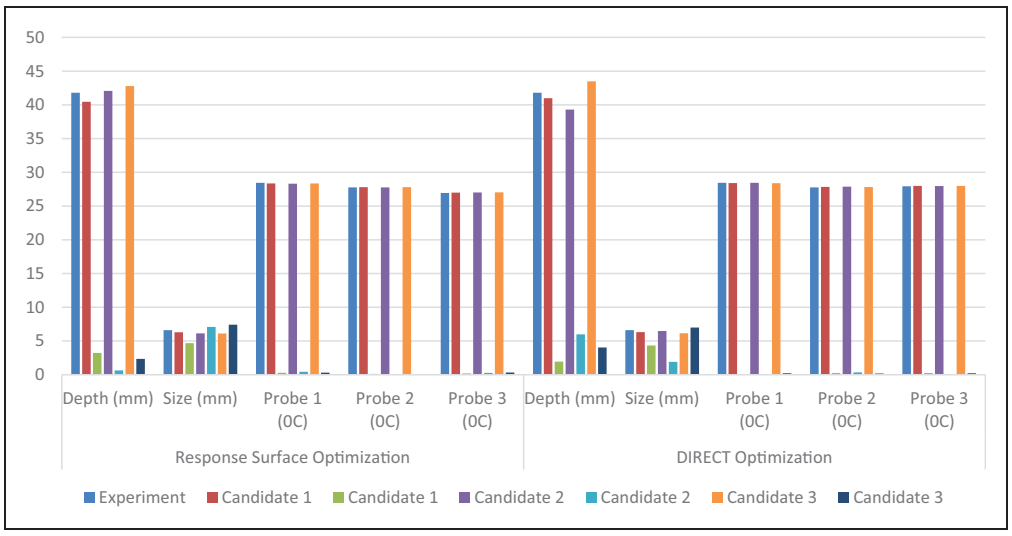

Figure 13. Comparison of the performances of two search methods for the reverse numerical simulations.

patients have breast tumor, who were named as cases No. 1 and No. 2.

By using the estimated tissue and blood perfusion parameters from healthy breasts through initial reverse simulation, further reverse thermal simulation was conducted to compute the sizes and depths of tumor. As in previous simulations, convergence studies were essential and carried out. It was found that when more parameters were searched in reverse thermal modeling using a more sophisticated breast model with blood perfusion based on patient specific data, the Genetic Algorithm (GA) was the most efficient design optimization method.

Figure 14 shows the fitness value versus generation number for the optimization process in search for size and depth of tumor for patient No. 1, which converged longer than parameter estimation, despite the number of populations is the same. In case 1, convergence was reached at around 40th generation. In backward simulation for patient case 2, the number of populations was set to 20 (Figure 15).

For the case where the number of populations was increased, convergence was achieved with early generations; however, this led to increment of iteration number and doubling the simulation time. The optimal parameters for Genetic Algorithm (GA) is to set generation number to 50 with a population of 10.

Reverse computational study results with GA for estimation of sizes and locations of tumor, was included in Table 6. Taking into account that the doctor's examination was performed only by palpation and given sizes are assumptions made during this procedure, the calculated results can be considered as having close agreement with the doctor's diagnosis. In the case of patient one, the computed size of tumor is around 30 mm, while it was reported by the doctor as 25 mm. The depth is about 3 cm from skin surface, which is close enough to be sensed by palpation. For patient two, the calculated diameter is about 8 mm, and located at 6 mm from skin surface, which can be validated by doctor's opinion where the tumor size is 5 mm and near to skin surface too.

Figure 16 presents a comparison of computed and measured temperature distributions for patient one with a tumor in the breast. In general, the distributions of temperature and locations of the hot spot

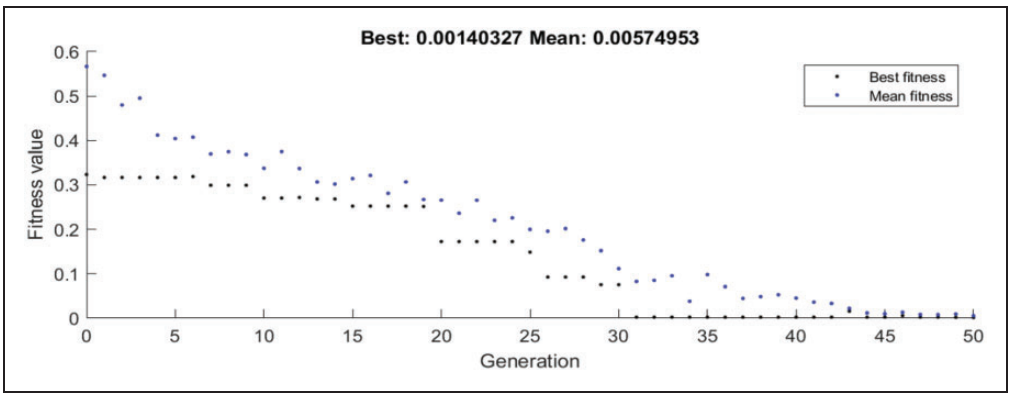

Figure 14. Fitness value vs generation with tumor (patient No. 1).

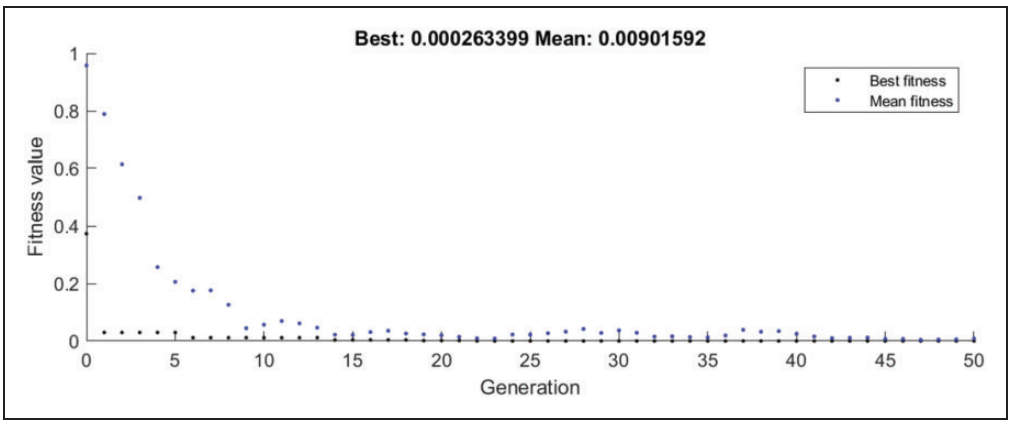

Figure 15. Fitness value vs generation with tumor (patient No. 2).

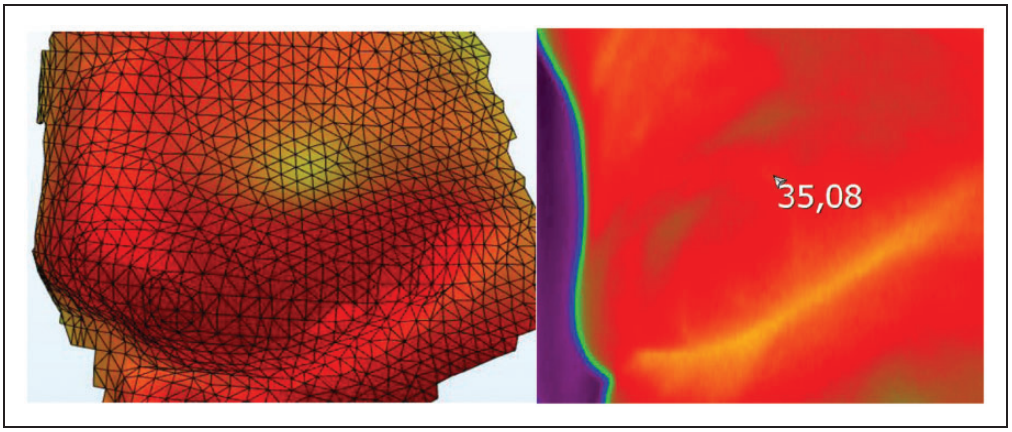

Figure 16. Comparison of computed and measured temperature distribution (patient No. 1).

match well. However, we can see the difference on the shape of the hotspot, which can be caused by non-uniformly distributed blood perfusion and vessels in the real breast, while the numerical model assumes uniform in their distributions. The temperature computed at the hotspot is 35.08 °C, which is validated by the breast hotspot measurement with the same temperature.

On the second patient's breast as shown in Figure 17, the computed and measured temperature distributions also match with each other in general, and the temperature at hotspot was calculated as 32.96 °C. Similarly it is noted that the computational model generates rather uniform temperature distribution compared to the measurement. In conclusion, the breast model was validated since the locations and

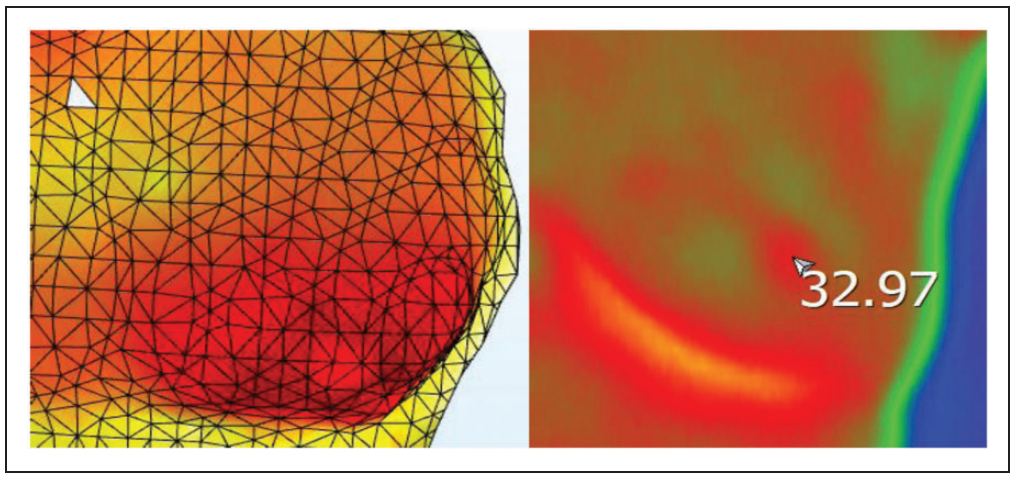

Figure 17. Comparison of computed and real temperature distribution (patient No. 2).

temperatures of the hotspots are comparable to the measurements.

Conclusion

In this study three methods were employed and tested for reverse modeling, and the results were validated by experiments with artificial breasts, and patient specific data. The numerical simulations were conducted by the use of DIRECT Optimization Method, Surface Response Optimization and Nelder-Mead techniques. The aim of the simulations was to find the depths and sizes of tumors in the breasts, which were measured in experiments for validation purpose. Based on the analysis and comparison of the results generated by the methods, it was concluded that the DIRECT Optimization was more accurate compared with the Surface Response Method, however it was more time consuming. The Nelder-Mead method could not converge to correct solutions. Therefore, the DIRECT optimization was preferred for the inverse modelling, but the computational time did not allow this method to be used extensively. It was concluded that the Response Surface Optimization method should be used first, and after proper ranges of the parameters were found, the DIRECT optimization method could be applied for more accurate results. However the GA method was found to be the only viable and efficient design optimization method for reverse modeling when blood perfusion was adopted in the breast model and many parameters were searched for with patient specific data input for breast tumor diagnosis. Subsequently this methodology was used for the reverse modelling with patient specific data and a blood perfusion model for tumor diagnosis and validation. It was revealed that the blood flow inside the breast is a very important factor and should be included in further simulations with clinical data. Based on temperature measurements and scanned geometry from the healthy breast for each patient, tissue thermal conductivity, density, specific heat and blood perfusion coefficients were estimated using reverse thermal modeling. Using those parameters and measured temperature distributions as well as the breast geometry from the diseased breast, the depth and size were computed in a further reverse modeling simulation. The predicted parameters had close agreement with the doctor's diagnostic results. Comparison of computed and measured temperature distributions showed reasonable agreement between them and the same values of temperature at hotspots were also found. However, as the numerical model assumes homogenous tissue properties and blood perfusion rate is constant in the simulations, there are minor differences in temperature variations, which can be due to the fact that a real breast consists of different layers with irregular transition with rather random locations of vessels which may create minor non-uniform distributions of heat.

The main disadvantage of the study is the use of a uniform breast model, therefore in the future it is planned to adopt a multi-layer model in the developed methodology to diagnose tumors in patients' breasts as well as to extract personalized tissue mechanical through the inverse thermal modeling. For this purpose, a large volume of patients' personalized data are being collected in an oncology hospital.

Acknowledgements

The authors thank Nazarbayev University Research and Innovation System for administrating the research project.

Declaration of Conflicting Interests

The author(s) declared no potential conflicts of interest with respect to the research, authorship, and/or publication of this article.

Funding

The author(s) disclosed receipt of the following financial support for the research, authorship, and/or publication of this article: The authors are grateful to Ministry of Education and Science of the Republic of Kazakhstan for financing this work through the grant for the "Development of an intelligent system for early breast tumor detection and cancer prediction" (AP05130923).

ORCID iD


Y Zhao https://orcid.org/0000-0002-9574-4787

References

1. Kennedy DA, Lee T and Seely D. A comparative review of thermography as a breast cancer screening technique. *Integr Cancer Ther* 2009; 8: 9–16.
2. American Cancer Society official website, www.cancer.org/cancer/cancer-in-young-adults/cancers-in-young-adults.html (accessed 9 December 2019).
3. Gautherie M and Gros CM. Breast thermography and cancer risk prediction. *Cancer* 1980; 45: 51–56.
4. Hatwar R and Herman C. Inverse method for quantitative characterization of breast tumours from surface temperature data. *Int J Hyperthermia* 2017; 33: 741–757.
5. Mitra S and Balaji C. A neural network based estimation of tumour parameters from a breast thermogram. *Int J Heat Mass Tran* 2010; 53: 4714–4727.
6. Tepper M, Shoval A, Hoffer O, et al. Thermographic investigation of tumor size, and its correlation to tumor relative temperature, in mice with transparable solid breast carcinoma. *J Biomed Opt* 2013; 18: 1114–1110.
7. Bezerra LA, Ribeiro RR, Lyra PRM, et al. An empirical correlation to estimate thermal properties of the breast and of the breast nodule using thermographic images and optimization techniques. *Int J Heat Mass Tran* 2020; 149: 1192–1115.
8. Espíndola NA, Bezerra LA, Santos LC, et al. Estimating breast thermophysical parameters by the use of mapping surface temperatures measured by infrared images. *IEEE Latin America Trans* 2018; 16: 2617–2624.
9. Das K and Mishra C. Non-invasive estimation of size and location of a tumor in a human breast using a curve fitting technique. *Int Commun Heat Mass Transfer* 2014; 56: 63–70.
10. Ferreira de Melo JR, Alves Queiroz JR, Bezerra LA, et al. Development of a three-dimensional surrogate geometry of the breast and its use in estimating the thermal conductivities of breast tissue and breast lesions based on infrared images. *Int J Commun Heat and Mass Transfer* 2019; 108: 1–9.
11. Ng EYK. A review of thermography as promising non-invasive detection modality for breast tumor. *Int J Sci* 2009; 48: 849–859.
12. Mital M and Pidaparti RM. Breast tumor simulation and parameters estimation using evolutionary algorithms. *Model Simul Eng* 2008; 2008: 1–6.
13. Das K and Mishra C. Simultaneous estimation of size, radial and angular locations of a malignant tumor in a 3D human breast – a numerical study. *J Therm Biol* 2015; 52: 147–156.
14. Ghassemi M and Shahidian A. *Nano and bio heat transfer and fluid flow*. Amsterdam: Elsevier, 2017.
15. Kumar PD, Kumar K and Rai N. A numerical study on dual-phase-lag model of bio-heat transfer during hyperthermia treatment. *J Therm Biol* 2015; 49-50: 98–105.
16. Lewis RM, Torczon V and Trosset MW. Direct search methods: then and now. *J Comput Appl Math* 2000; 124: 191–207.
17. Baeyens E, Herreros A and Peran JR. A direct search algorithm for global optimization. *Algorithms* 2016; 9: 401–422.
18. Cohn A, Scheinberg K and Vicente L. *Introduction to derivative-free optimization; MOS/SIAM series on optimization*. Philadelphia, PA: SIAM, 2009.
19. Shubert BO. A sequential method seeking the global maximum of a function. *SIAM J Numer Anal* 1972; 9: 379–388.
20. Sergeyev YD and Kvasov DE. Global search based on efficient diagonal partitions and a set of lipschitz constants. *SIAM J Optim* 2006; 16: 910–937.
21. Lera D and Sergeyev YD. Lipschitz and holder global optimization using space-filling curves. *Appl Numer Math* 2010; 60: 115–129.
22. Kvasov DE and Sergeyev YD. Lipschitz global optimization methods in control problems. *Autom Remote Control* 2013; 74: 1435–1448.
23. Jones DR, Perttunen CD and Stuckman BE. Lipschitzian optimization without the Lipschitz constant. *J Optim Theory Appl* 1993; 79: 157–181.
24. Solis FJ and Wets RJB. Minimization by random search techniques. *Mathematics OR* 1981; 6: 19–30.
25. Pearl J. *Heuristics: Intelligent search strategies for computer problem solving*. Boston, MA: Addison-Wesley Longman Publishing Co., Inc., 1984.
26. Holland JH. *Adaptation in natural and artificial systems*. Michigan: University of Michigan Press, 1975.
27. Yunker JM and Tew JD. Simulation optimization by genetic search. *Math Comput Simul* 1994; 37: 17–28.
28. Dennis J, Price C and Coope I. Direct search methods for nonlinearly constrained optimization using filters and frames. *Optim Eng* 2004; 5: 123–144.
29. Nelder JA and Mead RA. A simplex method for function minimization. *Comput J* 1965; 7: 308–313.
30. Spendley W, Hext GR and Himsworth FR. Sequential application of simplex designs in optimization and evolutionary operation. *Technometrics* 1962; 4: 441–4611.
31. Cao YJ and Wu QH. Teaching genetic algorithm using MatLab. *Int J Electr Eng Educ* 1999; 36: 139–153.